

Chapter 3: Reoptimization of the Berman (1983) CMAS Liquidus Model in Anorthite Phase Space

3.1 INTRODUCTION

Accurate thermodynamic interpretations of partitioning between minerals and melts and their successful application to igneous processes are heavily dependent on the quality of major-element activity-composition models of melts in the compositional systems of interest. This chapter describes a targeted effort to improve the Berman (1983) CaO-MgO-Al₂O₃-SiO₂ thermodynamic melt model for use in studies of anorthite partitioning, such as that discussed in chapter 2. New Margules parameters are reported for melts between 40 and 50 mol % SiO₂ on the anorthite liquidus that reduce discrepancies between experimentally measured liquidus temperatures and those calculated from the model by 35 %.

3.1.1 Description of Berman CMAS Thermodynamic Melt Model

Two main approaches exist for describing the molecular interactions that govern energies of solution in melt systems: speciation and stoichiometric models (for a more detailed overview, see Berman and Brown (1987)). Speciation models, which are mathematically more complicated, attempt to identify all, or at least a representative critical mass of, molecular species present in the melt and incorporate as much nonideal mixing behavior into speciation as possible. Usefulness of this approach is often limited by not knowing melt species identities well and the lack of standard state property data

for many of them, so full treatments have been limited to simple, well studied binaries such as $\text{Na}_2\text{O-SiO}_2$ (e.g., Halter and Mysen, 2004). Less rigorous variations of this approach in more complex systems have approximated melt structure as consisting of one species similar to a coexisting mineral phase of interest, as in Blundy et al. (1996), or “two-lattice” models (e.g., Drake, 1976; Nielsen and Dungan, 1983) that treat melts as being composed of two independent quasi-lattices, each an ideal solution: a network-forming lattice of SiO_2 and aluminous species MAlO_2 and MAl_2O_4 (where M = a monovalent or divalent cation) and a network-modifying lattice on which oxides such as CaO , MgO , and FeO are evenly distributed.

In contrast, a stoichiometric model makes no assumptions about melt structure and instead designates a number of endmember components that encompass the entire compositional field of interest. Calculating melt energetics using these endmembers as fictive melt species is generally more mathematically tractable and one has greater flexibility in choosing components for which thermodynamic data exists. The extent to which the chosen endmember species do not represent the actual species present in the melt can be reflected in extremely non-ideal mixing behavior of these species in the model. For example, the CaO activity coefficients calculated using the Berman (1983) stoichiometric model in the CMAS melts of chapter 2 are on the order of 10^{-5} , indicating that very little Ca inhabits these melts as a simple oxide. Use of one or more species such as CaSiO_3 , CaAl_2O_4 , or $\text{CaAl}_2\text{Si}_2\text{O}_8$ might account for a greater amount of the solution energy associated with Ca molecules via their molar proportions alone.

The Berman model (1983) uses simple neutral oxides as fixed endmember components and parameterizes melt activities for each oxide as a function of composition

and temperature, with enthalpy and entropy excess mixing terms (Margules parameters) fitted to liquidus relations. The Gibbs free energy of a solution can be described as the sum of two parts: the free energy associated from ideal mixing behavior of a species in the melt, which depends only on the concentration of the species, and the energy arising from non-ideal mixing, here termed “excess”:

$$\Delta G_{solution} = \Delta G_{ideal} + \Delta G_{excess} . \quad (3.1)$$

The excess Gibbs free energy of the system may be described with the following expression for any number (nc) of components (i), where X is the molar fraction, T is the absolute temperature, R is the gas constant, and γ is the activity coefficient:

$$\Delta G_{excess} = \sum_{i=1}^{nc} X_i RT \ln \gamma_i . \quad (3.2)$$

In the case of the quaternary system CaO-MgO-Al₂O₃-SiO₂ (CMAS), there are 31 different mixing combinations of the four end-member oxide components, with an enthalpy term (W_H) and entropy term (W_S) for each. The general Margules term, W , used in the model represents a simple relationship incorporating both, along with a temperature term. For a given combination of mixing components i , the expression for W is:

$$W_i = W_{H_i} - TW_{S_i} . \quad (3.3)$$

The Berman model empirically approximates liquid excess free energy of a liquid species using the general polynomial expression,

$$RT \ln \gamma_m = \sum_{i_1=1}^{nc-1} \sum_{i_2=i_1}^{nc} \dots \sum_{\substack{i_p=i_{p-1} \\ i_p \neq i_1}}^{nc} W_{i_1 i_2 \dots i_p} \left[Q_m X_{i_1} X_{i_2} \dots X_{i_p} / X_m + (1-p) X_{i_1} X_{i_2} \dots X_{i_p} \right] . \quad (3.4)$$

Here m is the oxide component of interest, p is the degree of polynomial, Q_m is the number of times the liquid oxide (m) appears in a particular mixing interaction, and X is the mole fraction of a component in the liquid of interest. The activity coefficient of oxide component m in a quaternary system may be calculated from the fourth degree polynomial expression of the general equation above:

$$\gamma_m = \exp \left[\left(\sum_{i_1=1}^3 \sum_{i_2=i_1}^4 \sum_{i_3=i_2}^4 \sum_{\substack{i_4=i_3 \\ i_4 \neq i_1}}^4 W_{i_1 i_2 i_3 i_4} \left[Q_m X_{i_1} X_{i_2} X_{i_3} X_{i_4} / X_m - 3 X_{i_1} X_{i_2} X_{i_3} X_{i_4} \right] \right) / RT \right]. \quad (3.5)$$

Instead of employing regression fitting to minimize residuals over the entire data set, the approach used in Berman model fits the data via linear programming to maintain the uncertainty consistency associated with each data point. Specifics of model calibrations are discussed in detail in Berman and Brown (1984) as well as Berman (1983).

3.2 MODEL PERFORMANCE

In order to more confidently quantify liquid thermodynamic effects on partitioning behavior for the data of chapter 2, it was highly desirable to determine the accuracy of the Berman CMAS model within the anorthite liquidus phase volume near the compositional range of seven CMAS compositions of interest (as shown in Figure 2.1). Model performance was evaluated by testing its ability to predict anorthite liquidus temperatures. Before proceeding, it should be noted that this work uses the correct values for ternary SAMM (SiO₂-Al₂O₃-MgO-MgO) interaction parameters that were printed as typos duplicating the values of SSAM reported in both the original thesis (1983) and De

Capitani and Brown (1987). The actual values for W_H and W_S for the SAMM interaction are 652384.49 and 397.38, respectively (J. Beckett, personal communication).

3.2.1 Calculating Anorthite-Melt Liquidus Temperatures from the Berman Model

At equilibrium on the anorthite liquidus, the chemical potential (μ) of pure anorthite equals the chemical potential of anorthite component in the coexisting melt phase, as shown in equation (3.6). The chemical potential of each phase is composed of both standard state (μ^0) and excess energy ($RT\ln a$) terms:

$$\sum_{i=1}^3 \rho_i \left[\mu_i^{o,Liq} + RT \ln(X_i^{Liq} \gamma_i^{Liq}) \right] = \mu_{anorthite}^o + RT \ln a_{anorthite} \quad (3.6)$$

The stoichiometric coefficient for oxide i in the anorthite formation reaction is represented by ρ_i . Activity coefficients for the liquid oxide components are calculated from equation (3.5), whereas the activity of anorthite of the solid phase is assumed equal to 1 (that is, the anorthite is assumed pure). Standard state chemical potential is described by the expression,

$$\mu^o = \Delta H_f^o + \int_{298.15}^T C_p dT - T \left[\Delta S^o + \int_{298.15}^T \frac{C_p}{T} dT \right]. \quad (3.7)$$

Heat capacities are calculated according to the following four term heat capacity equation used in Berman (1983):

$$C_p = A + CT^{-2} + DT^{-0.5} + FT^{-1} \quad (3.8)$$

The anorthite and liquid component heat capacity equation coefficients used are listed in Table 3.1.

Table 3.1. Anorthite and liquid oxide component standard state properties and heat capacity equation coefficients from Berman (1983).

	$\Delta H_f^{298.15, 1 \text{ bar}}$ J/mol	$\Delta S^{298.15, 1 \text{ bar}}$ J/mol	Heat capacity (C_p), J/mol·K			
			A	C	D	F
Anorthite	-4231480	199.90	422.521	-2189052	-3219.938	-
CaO liquid	-554897	26.228	76.044	-	-	-
Al ₂ O ₃ liquid	-1548481	102.785	154.820	-	-677.889	-8071.355
SiO ₂ liquid	-904927	45.000	121.630	-	-1444.383	-

The success of the Berman model can be assessed by comparing the liquidus temperatures it predicts for various melt compositions coexisting with pure anorthite with those observed experimentally for those compositions. The reported uncertainty in anorthite liquidus temperatures based on the calibration data used by Berman (Berman, 1983) for the 20 wt. % Al₂O₃ plane of the quaternary, near our region of interest, exceeded 20 °C. The need for an accurate set of liquid activity coefficient and anorthite liquidus temperatures for the experimental protocol described in chapter 2 of this thesis motivates our attempt at a Margules parameterization refinement specifically to reduce this uncertainty. Furthermore, a plot (Figure 3.2a) of liquidus temperature discrepancies between the model and experiments in which anorthite coexists with CMAS melts between 40–50 mol % SiO₂ revealed an positive correlation of the temperature residual with the melt CaO content. No similar systematic relationships between ΔT_L and the other melt oxide components MgO, Al₂O₃, and SiO₂ emerged. While these discrepancies generally fall within expected model performance, they suggest that some degree of melt

behavior is left unaccounted for by the Berman model that might be recovered by a targeted reoptimization of the model within our compositional range of interest.

3.3 REOPTIMIZATION OF BERMAN MODEL

3.3.1 Data Selection

A reoptimization of the Berman model was performed within the 40–50 mol % SiO₂ portion of the anorthite liquidus space in the system CMAS. This was accomplished by adjusting the Margules parameters to minimize the differences between the liquidus temperatures predicted by the model and those experimentally determined for anorthite in 57 CMAS liquids with SiO₂ content between 40 and 50 mol % (Chapter 2, Osborn, 1942; Osborn and Tait, 1952; Tsuchiyama, 1983; Yang et al., 1972). Compositions and observed liquidus temperatures are listed in Table 3.2. These data all constrained the anorthite liquidus to within 5 °C, thus offering sufficient precision for use in this modeling. Several other studies (Anderson, 1915; DeVries and Osborn, 1957; Osborn et al., 1954; Prince, 1954) contain an additional 61 points in CMAS-anorthite liquidus space, but the bulk of these data falls outside the composition region of interest and are thus not selected for this model reoptimization. DeVries and Osborn (1957) compositions all contain significantly more alumina, whereas the Anderson (1915), Osborn et al. (1954), and Prince (1954) data sets tend to have >50 % molar SiO₂.

Table 3.2. Literature anorthite-CMAS melt liquidus data from composition region ~40–50 mol % SiO₂.

Source	T _L , ° C*	X CaO	X MgO	X Al ₂ O ₃	X SiO ₂
CMAS2 (Chapter 2)					
	1403	0.207	0.159	0.151	0.483
	1408	0.228	0.142	0.144	0.487
	1408	0.250	0.119	0.141	0.490
	1408	0.277	0.093	0.137	0.493
	1400	0.300	0.068	0.134	0.498
	1401	0.322	0.040	0.133	0.504
	1398	0.345	0.014	0.132	0.508
Tsuchiyama (1983)					
	1270	0.257	0.160	0.089	0.494
	1360	0.253	0.122	0.126	0.499
Yang et al. (1972)					
	1257	0.281	0.187	0.102	0.431
	1276	0.263	0.196	0.110	0.432
	1264	0.282	0.183	0.103	0.432
	1252	0.288	0.178	0.102	0.432
	1299	0.258	0.190	0.117	0.435
	1294	0.269	0.180	0.115	0.436
	1254	0.313	0.149	0.102	0.436
	1304	0.276	0.164	0.120	0.439
	1335	0.260	0.169	0.130	0.441
	1355	0.281	0.134	0.136	0.448
	1399	0.241	0.149	0.158	0.452
	1366	0.311	0.094	0.140	0.455
	1411	0.277	0.104	0.160	0.460
	1443	0.233	0.116	0.186	0.465
	1437	0.267	0.091	0.176	0.466
Osborn and Tait (1952)					
	1325	0.192	0.218	0.128	0.461
	1448	0.201	0.130	0.201	0.468
	1305	0.202	0.211	0.119	0.468
	1444	0.216	0.122	0.186	0.477
	1392	0.216	0.148	0.158	0.478
	1353	0.217	0.172	0.132	0.478
	1296	0.218	0.196	0.108	0.479
	1291	0.221	0.195	0.103	0.481
	1288	0.225	0.194	0.098	0.483
	1287	0.228	0.186	0.101	0.485
	1280	0.228	0.191	0.096	0.485
	1498	0.232	0.048	0.232	0.488
	1280	0.234	0.187	0.089	0.490
	1297	0.237	0.177	0.094	0.492

Table 3.2. (continued)

Source	$T_L, ^\circ\text{C}^*$	X CaO	X MgO	X Al ₂ O ₃	X SiO ₂
Osborn (1942)	1239	0.333	0.084	0.083	0.500
	1263	0.328	0.084	0.087	0.500
	1258	0.342	0.070	0.088	0.500
	1288	0.371	0.029	0.101	0.500
	1323	0.250	0.141	0.109	0.500
	1333	0.276	0.113	0.110	0.500
	1337	0.303	0.086	0.111	0.500
	1333	0.330	0.058	0.112	0.500
	1328	0.358	0.029	0.113	0.500
	1323	0.386	0.000	0.114	0.500
	1388	0.250	0.115	0.135	0.500
	1393	0.277	0.087	0.136	0.500
	1398	0.305	0.059	0.137	0.500
	1398	0.333	0.030	0.138	0.500
	1438	0.250	0.089	0.161	0.500
	1463	0.335	0.000	0.165	0.500
	1488	0.250	0.061	0.189	0.500
	1498	0.279	0.031	0.191	0.500
	1510	0.308	0.000	0.192	0.500
	1533	0.250	0.031	0.219	0.500

* Where liquidus are bracketed by an experiment at temperature T_1 where only glass is present and T_2 where both anorthite and glass are observed, the liquidus is assumed to be the average of T_1 and T_2 .

3.3.2 Model Reoptimization Procedure and Results

The reoptimization process involved a very simple program making iterative adjustments to the 62 Margules parameters, term by term, to find new parameters that minimize the sum of squares of liquidus temperature differences between the observed experimental data set and those predicted by the evolving thermodynamic model. Specifically, the program changes a Margules parameter by increasing or decreasing it incrementally and recalculates the liquid oxide component activities according to the new parameter value. New liquidus temperatures are calculated after each parameter value

adjustment such that $\Delta\mu_{\text{anorthite}} = \Delta\mu_{\text{anorthite liquid}}$ for all the data compositions being modeled. When a minimum is found for the one-dimensional search along a given parameter direction (that is, when adjustments to the parameter value become smaller than 0.1% of the value), the program accepts the new value and proceeds to search for the optimum value of the next Margules parameter. This term-by-term search is not optimal for finding a global minimum in multi-parameter space, but that is not a reasonable goal when optimizing a 62-parameter model to 57 experimental constraints. Instead this computationally straightforward method is sufficient for seeking incremental improvements relative to the starting model without any claim to uniqueness of the solution.

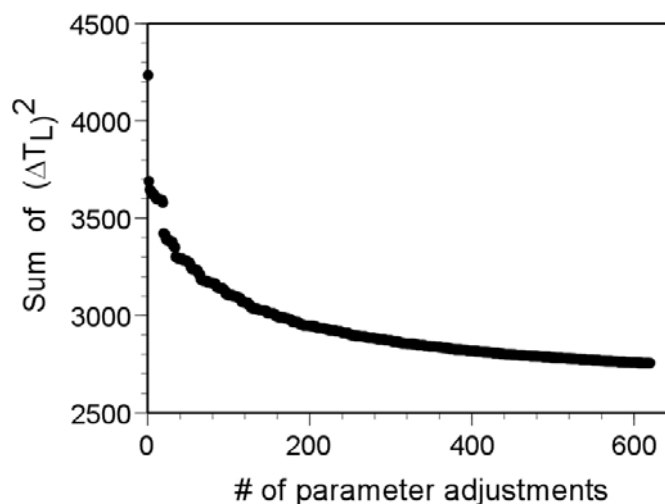


Figure 3.1. Reduction of the sum of differences squared between experimental measurements of liquidus temperatures and those calculated from the model $(\Delta T_L)^2$ as a function of the number of Margules parameter adjustments made during reoptimization of the Berman model.

It is important to recognize that this reoptimization considered only anorthite-melt constraints and is presumed to be worse than the original Berman model at describing not only equilibria with other solids but potentially portions of the anorthite liquidus outside the compositional range of experimental liquidus data selected. However, the reparameterization successfully eliminates the apparent systematic dependence of liquidus temperature errors on melt CaO content in this compositional region, as shown in Figure 3.2.

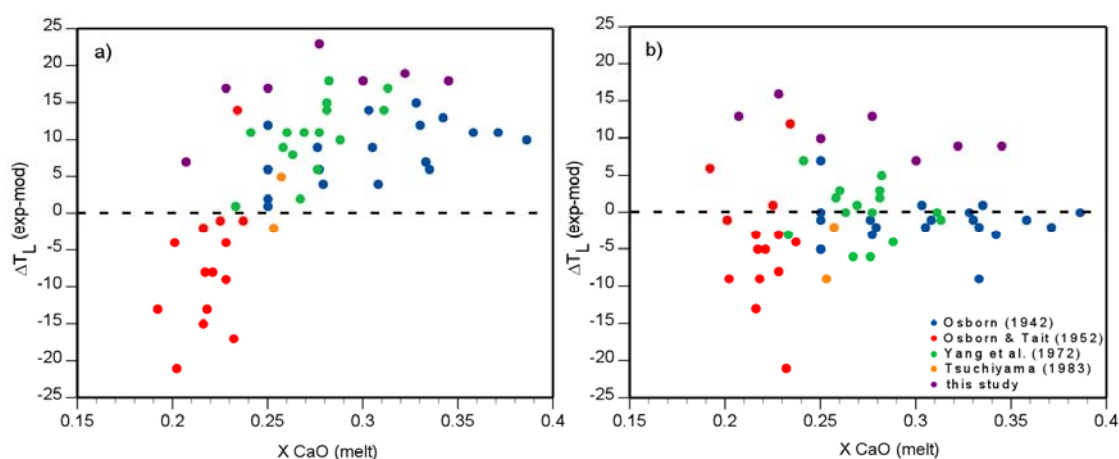


Figure 3.2. Difference between anorthite liquidus temperature (ΔT_L) as a function of molar melt CaO content as measured experimentally (exp) and calculated by thermodynamic model (mod): (a) Berman (1983) CMAS activity model, and (b) after reoptimization of Berman model using CMAS experimental literature data shown.

3.3.3 Discussion

Vulnerability to systematic errors is a known disadvantage of stoichiometric melt models (Beckett, 2002), and this effect can be significant when applying them to other thermodynamic modeling efforts. This is illustrated by the exercise in chapter 2 of this thesis, where the two sets of Margules parameters discussed here generate distinctly different predictions of Mg site occupancy (tetrahedral vs. octahedral/cubic) for

anorthites coexisting with CMAS melt compositions (see Figure 2.4). Molar D_{MgVIII} values calculated from the Berman model exceed those of the reoptimized model by a factor of ~ 3 . A detailed spectroscopic study of Mg site distribution in anorthite might definitively indicate whether the reoptimized melt model produces a more accurate description of Mg in the crystal structure. As no such site occupancy data currently exist, improvements in liquidus temperatures within a subregion of the anorthite phase volume remain the sole justification for using this reoptimization to thermodynamically rationalize the divalent cation partitioning data of chapter 2.